ACS APPLIED MATERIALS & INTERFACES

Research Article

www.acsami.org

Intercorrelation of Electronic, Structural, and Morphological Properties in Nanorods of 2,3,9,10-Tetrafluoropentacene

Sabine-A. Savu,[†,§] Andrea Sonström,[†,§] Rafael Bula,[‡] Holger F. Bettinger,[‡] Thomas Chassé,[†] and M. Benedetta Casu*[,†]

[†]Institute of Physical and Theoretical Chemistry and [‡]Institute of Organic Chemistry, University of Tübingen, Auf der Morgenstelle 18, D-72076 Tübingen, Germany

Supporting Information

ABSTRACT: We evidence the intercorrelation of electronic, structural, and morphological properties in nanorods of a substituted fluorine-based pentacene, 2,3,9,10-tetrafluoropentacene, deposited on gold single crystals by using photoemission and X-ray absorption spectroscopy investigations. Our investigations show changes in the XPS spectroscopy lines, and NEXAFS features correlate with the specific structure of the assemblies and their morphology. Consequently, the chemical structure affects not only the molecular electronic structure and the way the molecules assemble in a film but also the film morphology leading to specific thin film electronic properties.

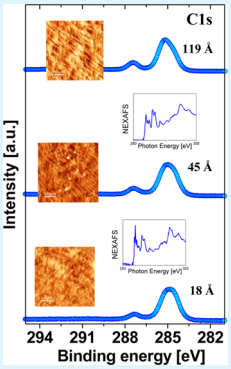

KEYWORDS: *electronic structure, X-ray photoelectron spectroscopy, X-ray absorption spectroscopy, atomic force microscopy, morphology, structure*

INTRODUCTION

Organic semiconductors have shown almost unprecedented success in reaching the market,[1] once the first device was proved.[2] Their properties are very attractive for their use in a large number of applications where low costs, chemical flexibility, and energy saving technologies play the major role: The plastic-based technology has still immense potential in functionalities, such as clothes, food labels, badges, and smart cards.[3] One of the greatest strengths of organic semiconductors is their chemical flexibility by synthesis: The concepts of chemical surface engineering[4] and design of organic semiconductors[5] are proven to be feasible ways to fully explore the technological opportunities offered by this class of materials. In this view, substitution is an efficient approach to pursue the goal of tuning important parameters, such as the gap between the highest occupied molecular orbital (HOMO) and the lowest unoccupied molecular orbital (LUMO), ionization potential, electron affinity, and transport properties in organic materials:[6] Unsubstituted pentacene (PEN), a p-type semiconductor, is the subject of numerous investigations owing to its high charge-carrier mobility and its ability to form highly oriented thin films.[7−15] Thus, substituted pentacenes enhancing pentacene properties, are very popular.[16−23] Here, we investigate the impact of functionalization on thin film characteristics (electronic properties, structure, and morphology), choosing 2,3,9,10-tetrafluoropentacene[24] (F4PEN, Figure 1), a fluorinated pentacene derivative, as a model system.

We investigate F4PEN nanorods deposited on Au(110) single crystals by using X-ray photoelectron spectroscopy (XPS), ultraviolet photoelectron spectroscopy (UPS), near edge X-ray absorption fine structure (NEXAFS) spectroscopy, and atomic force microscopy (AFM). The simultaneous use of this variety of techniques is coupled to the controlled in situ deposition, in order to avoid possible artifacts and discrepancies due to a noncompletely controlled environment that could affect our results.[25−27]

EXPERIMENTAL SECTION

Sample preparation and photoemission experiments were performed in an ultrahigh-vacuum (UHV) system consisting of two preparation chambers (base pressure, better than 10^{-9} mbar) and an analyzing chamber (base pressure, 8×10^{-10} mbar) equipped with a Specs Phoibos 150 analyzer, a monochromatic Al Kα source, and a high-flux He discharge lamp (UVS 300 Specs) with an excitation energy of 21.22 eV. The He I β and He I γ satellites were subtracted from the experimental data for all UPS spectra. The UPS experimental resolution (200 meV) was calculated from the broadening of the Fermi edge. A clean Au(110) single crystal (Surface Preparation Laboratory) was used as a substrate, prepared by several cycles of sputtering (Ar^+ ion bombardment, 1250 V) and annealing (600 K). The cleaning cycles were repeated until XPS, UPS, and low-energy electron diffraction showed no traces of contaminants. F4PEN was

Received: June 24, 2015
Accepted: August 19, 2015
Published: August 19, 2015

DOI: 10.1021/acsami.5b05622
ACS Appl. Mater. Interfaces 2015, 7, 19774−19780

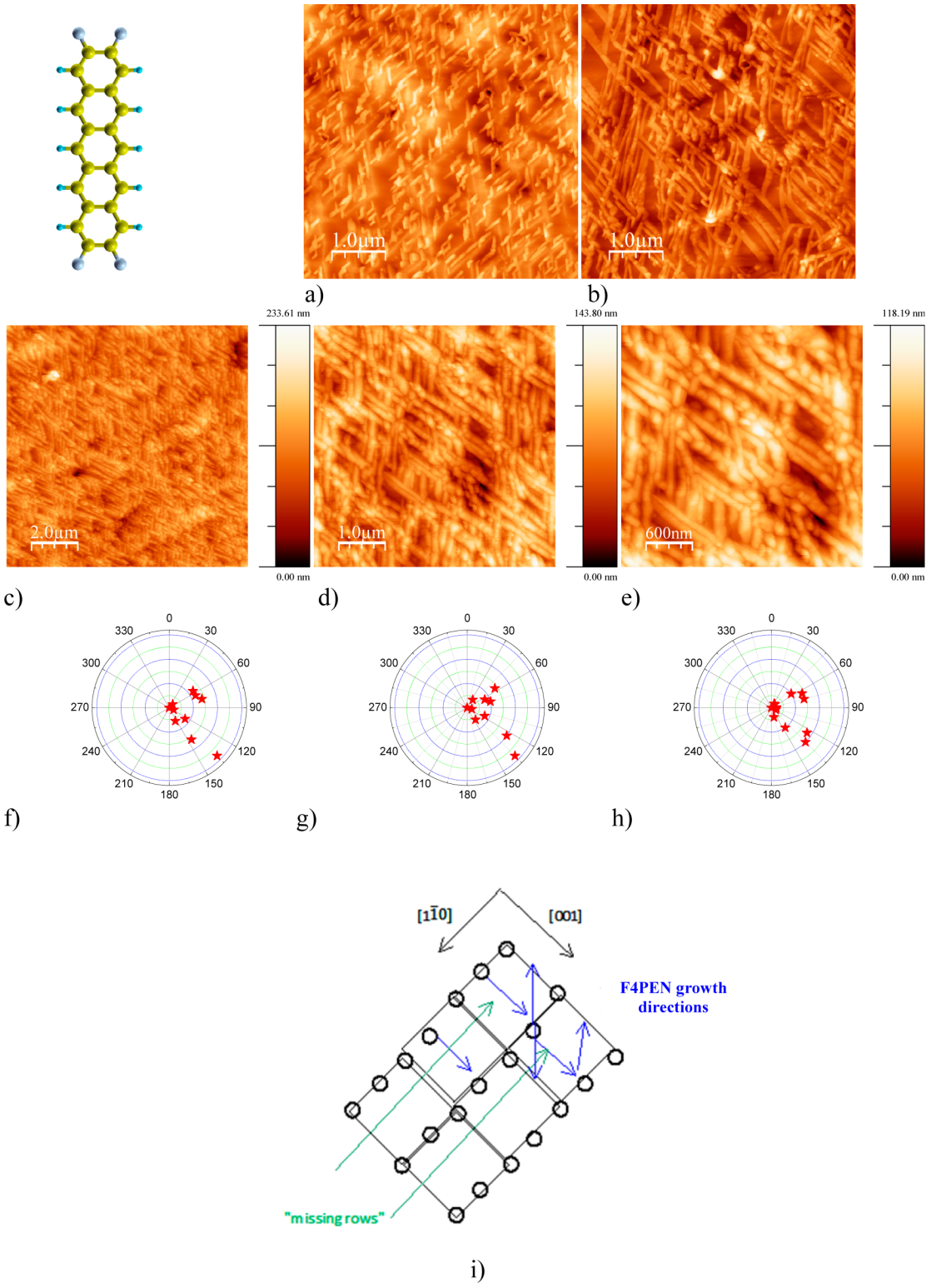

Figure 1. 5 μm × 5 μm AFM images of a nominally (a) 18 Å thick and (b) 40 Å thick nanorod assembly. (c) 10 μm × 10 μm, (d) 5 μm × 5 μm, and (e) 3 μm × 3 μm AFM images of a nominally 120 Å thick nanorod assembly; together with their relative nanorod angular dispersions: f, g, and h. (i) Sketch of the preferential nanorod growth directions on Au(110) single crystals. The F4PEN molecular structure is also shown (yellow indicates carbon atoms, blue indicates hydrogen atoms, and gray indicates fluorine atoms).

synthesized " in house" according to the route reported in ref 24. The preparation of the nanorods was carried out in situ under UHV conditions by using organic molecular beam deposition (evaporation rate, 1.3 Å/min; substrate at room temperature, T_{sub} = 300 K). The evaporation rate was measured with a quartz crystal microbalance. NEXAFS measurements were carried out at the UE52-PGM undulator beamline at BESSY (Berlin) in single bunch (top up mode; ring current = 13.6 mA; c_{ff} = 2.5; 40 μm exit slit; analyzer resolution = 0.1 eV). The main chamber (base pressure, 2 × 10^{10} mbar) was equipped with a standard twin anode X-ray source and a SCIENTA R4000 electron energy analyzer. We carried out NEXAFS measurements in the partial electron yield mode, in grazing incidence (70° with respect

DOI: 10.1021/acsami.5b05622
ACS Appl. Mater. Interfaces 2015, 7, 19774−19780

to (wrt) the sample normal). The NEXAFS spectra were normalized by using the clean substrate signal and the ring current. All spectra were scaled to give an equal edge jump. Details on NEXAFS normalization are given elsewhere.[10,28] No degradation of the samples was observed on the time scale of all discussed experiments. AFM measurements (Digital Instruments Nanoscope III Multimode) were performed under ambient conditions in tapping mode.

RESULTS AND DISCUSSION

F4PEN molecules (F4PENs) form, under the present preparation conditions, islands appearing as nanorods (see Figure 1). This morphology also characterizes the assemblies of other substituted pentacenes.[22,23] On average, with increasing nominal thickness of the F4PEN assembly, the nanorods become longer, while the height distribution does not change relevantly (see the Supporting Information). This effect, as well as the nanorod-type morphology, is due to the fact that the barriers to surface diffusion on a terrace are anisotropic: Diffusing across the width of a nanorod involves energy barriers twice as high as diffusing along its length, favoring the formation of nanorods.[23] The nanorods do not grow randomly distributed on the Au(110) surfaces; only certain directions are favored. Analyzing the AFM images we find that they preferentially grow along the direction perpendicular to the missing-row reconstruction in a Au(110) single crystal, i.e., along the [001]-direction, or, alternatively, forming a 60°/120° angle with respect to the [001]-direction (see nanorod angular dispersions and sketch in Figure 1). This behavior was previously observed for PENs on gold single crystals with the same substrate lattice geometry.[29] It is related to the geometry of the lattice substrate that can steer the aggregation of islands/nanorods during their growth.[30,31]

F4PENs are physisorbed on Au(110).[32] The C 1s and F 1s XPS core-level spectra of the thicker assembly are characterized by a peak at 285.2 and a peak at 687.7 eV, respectively (Figure 2). These main features are assigned in the C 1s core-level spectra (Figure 1a) to carbon atoms bound only to carbon or also to hydrogen, while the F 1s spectra show only a single line (Figure 2b), as expected because the fluorine atoms have the same chemical environment. A further peak at 287.5 eV, related to carbon atoms which are bonded to fluorine (CF), is visible in the C 1s spectra (Figure 2a).[32] We observe a thickness-dependent shift of the main lines toward higher binding energies with respect to the thinnest assembly main line (0.7 eV for the C 1s main line and 0.6 eV for the F 1s main line). The line shift is not only thickness-dependent but also nonrigid, as it is shown in Figure 2b. We observe two thickness regions: A first region with increasing energy shifts up to around 25 Å and a region above 25 Å, where the shifts almost stabilize. The nonrigid shift can be traced back to a fractional charge transfer from the metal to the molecules.[32] However, this does not explain the thickness-dependent difference of the main line shape that is particularly evident between 18 and 45 Å (Figure 2a).

To understand the reasons that may cause this phenomenon, it is important to identify and discuss the aspects that influence the electronic structure in F4PEN nanorods. NEXAFS signals are sensitive to the orientation of the molecules in the films, and the average molecular orientation can be directly calculated from the NEXAFS spectra, measured for at least two different polarizations of the incident light.[33] F4PENs experience a molecular reorientation with increasing thickness: A quantitative analysis performed on the π^* resonance at 286.1 eV

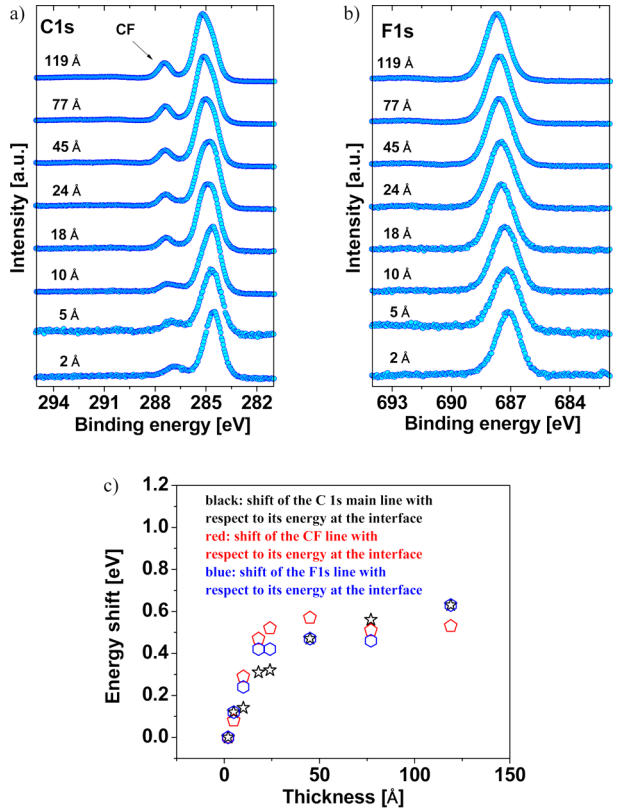

Figure 2. (a) Thickness-dependent C 1s and (b) F 1s core-level spectra of F4PEN assemblies. (c) Core-level shifts versus thickness of the C 1s and F 1s main lines and CF contribution, as indicated.

(Figure 3) yields an average tilt angle of the molecular plane with respect to the substrate of 31° for the thickest assemblies, while F4PENs are flat lying at the interface with gold. This is typical in thin films of organic small molecules when the influence of the substrate becomes less strong due to the larger distance from the interface. Indeed, if we consider two molecules, one close to the other, the way they would structurally assemble is determined by a compromise between the strength of the C−H and the $\pi-\pi$ interactions.[34] In a film or in a rod they are not isolated: They interact with the surrounding molecules that also aim at minimizing their energy because of the same interactions. In addition, the molecules interact with and feel the substrate potential. The consequence is the tendency of the molecules to assemble following the herringbone structure, and a large variety of thin film polymorphisms are reported in the literature.[8,34−36] The herringbone motif explains the characteristic NEXAFS dichroism behavior that we find for F4PENs, as this structure gives rise to contributions to both polarizations in the NEXAFS experiment.

The reorientation of the F4PENs in the nanorods generates a slightly different ionization potential[37] (I_P) for different thicknesses of the nanorods. We expect that this contributes rigidly to the shift observed in Figure 2c. Once the molecular orientation reaches the equilibrium values of the "thin film phase", beyond the influence of the substrate potential, the nanorod ionization potential stabilizes (see Supporting Information for the plot of I_P versus thickness). This is mirrored by the stabilization of the XPS line shifts in the range above 50 Å (Figure 2c). The change in ionization potential is 0.26 eV. Note that in ordered thin films of PEN the I_P

DOI: 10.1021/acsami.5b05622
ACS Appl. Mater. Interfaces 2015, 7, 19774−19780

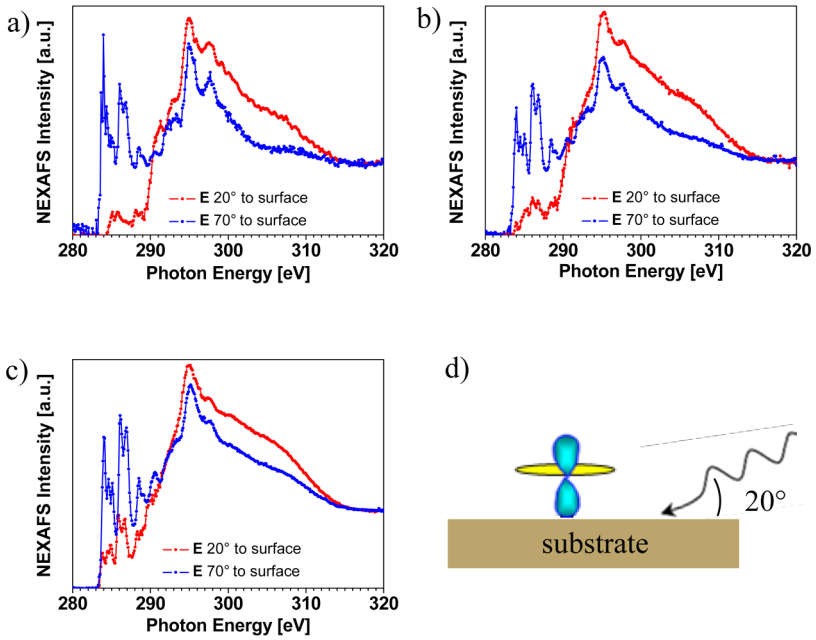

Figure 3. C K-NEXAFS spectra for nominal thicknesses of (a) 20, (b) 40, and (c) 175 Å measured for two different polarizations of the incoming light, as indicated. (d) Sketch of the NEXAFS experiment geometry.

difference between flat and standing molecules is 0.4 eV,[37] whereas it is 0.85 eV for PFP.[38] Therefore, F4PEN values are in agreement with the intermediate fluorination degree of F4PEN and the fact that in thicker assemblies F4PENs do not assume a standing configuration with respect to the substrate.

Comparing the NEXAFS spectra for different thicknesses, they show the structural effects due to the reorientation of the molecules that affects the resonance intensities, as discussed. In addition, the different energy onset between the thinner and the thicker assemblies is due to the charge transfer from the metal to the molecule, as discussed in ref 32. These two are not the only visible effects: At intermediate thicknesses we observe that the NEXAFS spectra are different from the spectra obtained at or far from the interface (compare Figure 3a–c). A similar behavior was observed for different diindenoperylene (DIP) film structures deposited on gold[27] and on silver,[39] and PEN deposited on PEDOT-PSS.[10] Indeed, changes in structure influence the electronic properties of the films, as seen for the orientation dependence of I_p.[37] Structurally ordered DIP thin films with different diffraction patterns have distinct valence level spectra, characterized by different peak positions, line widths, and relative intensities that correlate with the degree of order and the molecular orientation.[39] The investigation of optical properties in PFP thin films shows that the singlet exciton fission process strongly depends on the intermolecular coupling, that is, on the crystalline molecular packing.[40] Generally, structural properties impact on device performance.[41] Thus, we conclude that the difference in the thickness-dependent NEXAFS spectra not only has structural reasons but is also due to the difference induced in the unoccupied electronic states by those same structural differences.

The last aspect that we intend to analyze in this context is the assembly morphology. The AFM image of a nominally 18 Å thick assembly is characterized by isolated nanorods that, as previously discussed, grow following two specific directions (Figure 1a). With increasing the thickness of the assembly, the nanorods are not isolated (see the AFM image in Figure 1b), but they grow forming parallel assemblies of rods. We observe this specific morphology in the same thickness range that corresponds to a particularly round-shaped C 1s XPS main line (see Figure 2a, the C 1s spectra for 18 and 24 Å thicknesses), indicating a correlation between the two phenomena. This assembly morphology may give rise to specific interactions between the single F4PEN nanorods that consequently influence the XPS line shape. When the assembly thickness is high enough, this specific interaction is smeared by the overall contributions and the XPS line shape comes back to the initial "pointed" shape. Note that there is no change in the stoichiometry dependence of the XPS signal for the various films: They all fulfill the "intact molecule" requirement,[32,42] Solid state effects on the XPS line shape and shake up intensities are reported in the literature when comparing solid state and gas phase spectra of several small molecules;[26,43−45] however, this information was not yet correlated to morphological investigation.

CONCLUSIONS

In conclusion, our multitechnique approach clearly indicates the existence of a mutual correlation among electronic properties, structure, and morphology in F4PEN nanorods. We have discussed in the previous section the differences in I_P for F4PEN, PEN, and PFP, respectively: F4PEN I_p values agree with the intermediate degree of fluorination and the herringbone motif in the F4PEN nanorods.

Although the effect of functionalization on electronic and structural properties, in particular by fluorination, was already known,[46−49] we find that it impacts also on the morphological properties of the thin films. This intercorrelation is particularly evident when analyzing the extensive work on PEN and PFP published in the literature in light of our results. As a matter of fact, the most striking differences involve film morphology. Pentacene is known to grow on a variety of substrates and different preparation conditions following layer-by-layer (Frank-van der Merwe) or layers-plus-islands (Stranski-Krastnov) growth modes, with dendritic or compact large

DOI: 10.1021/acsami.5b05622
ACS Appl. Mater. Interfaces 2015, 7, 19774−19780

islands.[13,50,51] On the contrary, PFP exhibits lamellar or rod island shape,[52,53] while there is no evidence for smooth films.[52] Indeed, pentacene has no barriers to surface diffusion and a Schwoebel barrier of 7 kcal/mol.[23,54] Specific substitutions, increasing both barriers, influence the growth processes in its derivatives,[23] favoring the nanorod formation, also typical for F4PEN. This can be understood in terms of different degrees of steric hindrance; for example in pentacene with a methoxy group as a substituent the steric hindrance is higher than in fluorine-substituted pentacenes.[23]

Finally, it is also important to understand if this intercorrelation has general relevance. In this respect, we have analyzed the published results regarding phthalocyanines (Pcs) and perylene derivatives. This analysis confirms that our observation is not peculiar to the pentacene family, but it is a general pattern in organic thin films. For example, CoPc, CuPc and their fluorinated counterparts show pronounced differences in the electronic and structural properties of their thin films;[55] additionally, their morphology is remarkably different, also for preparation at different substrate temperatures.[56]

Perylene derivatives show the same intercorrelation effects. 3,4,9,10-Perylentetracarboxylic acid dianhydride (PTCDA), and DIP are among the most well-known and investigated examples, with PTCDA and DIP forming well-organized and stable films,[57−62] and DIP having very good transport properties.[63] PTCDA thin films can be grown up to the relevant number of 1000 layers keeping the molecular orientation parallel to the substrate,[64] DIP shows a transition from well-organized upright-standing to well-organized flat-lying molecules above 170 Å thickness (i.e., around nine layers).[61] Their island shape is also different: Sub-monolayers of PTCDA form islands that have a quadratic shape on Ag(100),[59,65] and sub-monolayers of PTCDA deposited on Ag(111) are characterized by dendritic islands[66] (Ag(100) at 120 K and Ag(111) at 100 K). DIP does not show a similar island morphology deposited on Ag(111) at 77 K.[67] Its branched film morphology is obtained, on the contrary, at higher substrate temperatures on Au(111) single crystals.[26,31]

Recently perylene diimide (PDI) derivatives became popular in view of their use in devices and have been proved to yield excellent stable n-channel OFETs.[68,69] Also PDI derivatives show a variety of structures and morphologies depending on substitutions,[70−72] further enhanced by their solution processability.[73−79]

Our present work and the preceding discussion undoubtedly show that the intercorrelation of electronic, structural, and morphological properties is a general feature and it has to be taken into account when designing new molecules or functionalizing existing ones, because a change in the chemical structure affects not only the molecular electronic structure but also the film morphology and the way the molecules assemble in a film, leading to specific/different thin films electronic properties.

On the other hand, this also represents an opportunity in order to achieve high-performing devices: Chemical changes in a molecule can be introduced, not only to change the electronic and the structural properties but also to create the desired film morphology, or it may be exploited as a tool for molecular patterning of surfaces. This certainly will have an impact on the device performance when the molecules are designed for technological applications.

■ ASSOCIATED CONTENT

Supporting Information

The Supporting Information is available free of charge on the ACS Publications website at DOI: 10.1021/acsami.5b05622.

Ionization potential versus thickness and AFM images and evaluation for three different assemblies (nominal thicknesses of 18, 40, and 119 Å) (PDF)

■ AUTHOR INFORMATION

Corresponding Author

*E-mail: benedetta.casu@uni-tuebingen.de. Tel.: +49 7071 29 76252. Fax: +49 7071 29 5490.

Author Contributions

§S.-A.S. and A.S. contributed equally to this work.

Notes

The authors declare no competing financial interest.

■ ACKNOWLEDGMENTS

We thank the Helmholtz-Zentrum Berlin (HZB), electron storage ring BESSY II, for providing beamtime, the HZB resident staff for beamtime support, and S. Pohl, W. Neu, and E. Nadler for technical support. Financial support from the Helmholtz-Zentrum Berlin is gratefully acknowledged. M.B.C. acknowledges the support of DFG through Contracts CA852/5-1 and CA852/5-2.

■ REFERENCES

(1) Forrest, S. R. The Road to High Efficiency Organic Light Emitting Devices. *Org. Electron.* **2003**, *4*, 45−48.

(2) Tang, C. W.; VanSlyke, S. A. Organic Electroluminescent Diodes. *Appl. Phys. Lett.* **1987**, *51*, 913−915.

(3) Plastic Fantastic. *Nature* **2013**, *499*, 379 (Editorial).10.1038/499379a

(4) Heimel, G.; Duhm, S.; Salzmann, I.; Gerlach, A.; Strozecka, A.; Niederhausen, J.; Burker, C.; Hosokai, T.; Fernandez-Torrente, I.; Schulze, G.; Winkler, S.; Wilke, A.; Schlesinger, R.; Frisch, J.; Broker, B.; Vollmer, A.; Detlefs, B.; Pflaum, J.; Kera, S.; Franke, K. J.; Ueno, N.; Pascual, J. I.; Schreiber, F.; Koch, N. Charged and Metallic Molecular Monolayers through Surface-Induced Aromatic Stabilization. *Nat. Chem.* **2013**, *5*, 187−194.

(5) Heimel, G.; Salzmann, I.; Duhm, S.; Koch, N. Design of Organic Semiconductors from Molecular Electrostatics. *Chem. Mater.* **2011**, *23*, 359−377.

(6) Wang, C.; Dong, H.; Hu, W.; Liu, Y.; Zhu, D. Semiconducting Π-Conjugated Systems in Field-Effect Transistors: A Material Odyssey of Organic Electronics. *Chem. Rev. (Washington, DC, U. S.)* **2012**, *112*, 2208−2267.

(7) Witte, G.; Woll, C. Growth of Aromatic Molecules on Solid Substrates for Applications in Organic Electronics. *J. Mater. Res.* **2004**, *19*, 1889−1916.

(8) Ambrosch-Draxl, C.; Nabok, D.; Puschnig, P.; Meisenbichler, C. The Role of Polymorphism in Organic Thin Films: Oligoacenes Investigated from First Principles. *New J. Phys.* **2009**, *11*, 125010.

(9) Ruiz, R.; Mayer, A. C.; Malliaras, G. G.; Nickel, B.; Scoles, G.; Kazimirov, A.; Kim, H.; Headrick, R. L.; Islam, Z. Structure of Pentacene Thin Films. *Appl. Phys. Lett.* **2004**, *85*, 4926−4928.

(10) Casu, M. B.; Cosseddu, P.; Batchelor, D.; Bonfiglio, A.; Umbach, E. A High-Resolution near-Edge X-Ray Absorption Fine Structure Investigation of the Molecular Orientation in the Pentacene/Poly(3,4-Ethylenedioxythiophene):Poly(Styrenesulfonate) Pentacene/System. *J. Chem. Phys.* **2008**, *128*, 014705−014705.

(11) Schreiber, F. Organic Molecular Beam Deposition: Growth Studies Beyond the First Monolayer. *Phys. Status Solidi A* **2004**, *201*, 1037−1054.

DOI: 10.1021/acsami.5b05622
ACS Appl. Mater. Interfaces 2015, 7, 19774−19780

(12) Dimitrakopoulos, C. D.; Malenfant, P. R. L. Organic Thin Film Transistors for Large Area Electronics. *Adv. Mater.* **2002**, *14*, 99−117.
(13) Ruiz, R.; Choudhary, D.; Nickel, B.; Toccoli, T.; Chang, K.-C.; Mayer, A. C.; Clancy, P.; Blakely, J. M.; Headrick, R. L.; Iannotta, S.; Malliaras, G. G. Pentacene Thin Film Growth. *Chem. Mater.* **2004**, *16*, 4497−4508.
(14) Witte, G.; Wöll, C. Molecular Beam Deposition and Characterization of Thin Organic Films on Metals for Applications in Organic Electronics. *Phys. Status Solidi A* **2008**, *205*, 497−510.
(15) Nabok, D.; Puschnig, P.; Ambrosch-Draxl, C.; Werzer, O.; Resel, R.; Smilgies, D.-M. Crystal and Electronic Structures of Pentacene Thin Films from Grazing-Incidence X-ray Diffraction and First-Principles Calculations. *Phys. Rev. B: Condens. Matter Mater. Phys.* **2007**, *76*, 235322.
(16) Anthony, J. E.; Brooks, J. S.; Eaton, D. L.; Parkin, S. R. Functionalized Pentacene: Improved Electronic Properties from Control of Solid-State Order. *J. Am. Chem. Soc.* **2001**, *123*, 9482−9483.
(17) Anthony, J. E.; Eaton, D. L.; Parkin, S. R. A Road Map to Stable, Soluble, Easily Crystallized Pentacene Derivatives. *Org. Lett.* **2002**, *4*, 15−18.
(18) Sheraw, C. D.; Jackson, T. N.; Eaton, D. L.; Anthony, J. E. Functionalized Pentacene Active Layer Organic Thin-Film Transistors. *Adv. Mater.* **2003**, *15*, 2009−2011.
(19) Chang, J.-F.; Sakanoue, T.; Olivier, Y.; Uemura, T.; Dufourg-Madec, M.-B.; Yeates, S. G.; Cornil, J.; Takeya, J.; Troisi, A.; Sirringhaus, H. Hall-Effect Measurements Probing the Degree of Charge-Carrier Delocalization in Solution-Processed Crystalline Molecular Semiconductors. *Phys. Rev. Lett.* **2011**, *107*, 066601.
(20) Chernick, E. T.; Casillas, R.; Zirzlmeier, J.; Gardner, D. M.; Gruber, M.; Kropp, H.; Meyer, K.; Wasielewski, M. R.; Guldi, D. M.; Tykwinski, R. R. Pentacene Appended to a TEMPO Stable Free Radical: The Effect of Magnetic Exchange Coupling on Photoexcited Pentacene. *J. Am. Chem. Soc.* **2015**, *137*, 857−863.
(21) Kawanaka, Y.; Shimizu, A.; Shinada, T.; Tanaka, R.; Teki, Y. Using Stable Radicals to Protect Pentacene Derivatives from Photodegradation. *Angew. Chem., Int. Ed.* **2013**, *52*, 6643−6647.
(22) Savu, S.-A.; Casu, M. B.; Schundelmeier, S.; Abb, S.; Tonshoff, C.; Bettinger, H. F.; Chassé, T. Nanoscale Assembly, Morphology and Screening Effects in Nanorods of Newly Synthesized Substituted Pentacenes. *RSC Adv.* **2012**, *2*, 5112−5118.
(23) Savu, S. A.; Abb, S.; Schundelmeier, S.; Saathoff, J. D.; Stevenson, J. M.; Tönshoff, C.; Bettinger, H. F.; Clancy, P.; Casu, M. B.; Chassé, T. Pentacene-Based Nanorods on Au(111) Single Crystals: Charge Transfer, Diffusion, and Step-Edge Barriers. *Nano Res.* **2013**, *6*, 449−459.
(24) Bula, R. P.; Oppel, I. M.; Bettinger, H. F. Thermal Generation of Pentacenes from Soluble 6,13-Dihydro-6,13-Ethenopentacene Precursors by a Diels−Alder-Retro-Diels−Alder Sequence with 3,6-Disubstituted Tetrazines. *J. Org. Chem.* **2012**, *77*, 3538−3542.
(25) Venables, J. A. *Introduction to Surface and Thin Film Processes*; Cambridge University Press: Cambridge, U.K., 2000.
(26) Casu, M. B.; Schuster, B.-E.; Biswas, I.; Raisch, C.; Marchetto, H.; Schmidt, T.; Chassé, T. Locally Resolved Core-Hole Screening, Molecular Orientation, and Morphology in Thin Films of Diindenoperylene Deposited on Au(111) Single Crystals. *Adv. Mater.* **2010**, *22*, 3740−3744.
(27) Casu, M. B. Nanoscale Order and Structure in Organic Materials: Diindenoperylene on Gold as a Model System. *Cryst. Growth Des.* **2011**, *11*, 3629−3635.
(28) Casu, M. B.; Scholl, A.; Bauchspiess, K. R.; Hubner, D.; Schmidt, T.; Heske, C.; Umbach, E. Nucleation in Organic Thin Film Growth: Perylene on $Al_2O_3/Ni_3Al(111)$. *J. Phys. Chem. C* **2009**, *113*, 10990−10996.
(29) Menozzi, C.; Corradini, V.; Cavallini, M.; Biscarini, F.; Betti, M. G.; Mariani, C. Pentacene Self-Aggregation at the Au(110)-(1 × 2) Surface: Growth Morphology and Interface Electronic States. *Thin Solid Films* **2003**, *428*, 227−231.
(30) Simbrunner, C.; Nabok, D.; Hernandez-Sosa, G.; Oehzelt, M.; Djuric, T.; Resel, R.; Romaner, L.; Puschnig, P.; Ambrosch-Draxl, C.; Salzmann, I.; Schwabegger, G.; Watzinger, I.; Sitter, H. Epitaxy of Rodlike Organic Molecules on Sheet Silicates—a Growth Model Based on Experiments and Simulations. *J. Am. Chem. Soc.* **2011**, *133*, 3056−3062.
(31) Casu, M. B.; Savu, S. A.; Schuster, B. E.; Biswas, I.; Raisch, C.; Marchetto, H.; Schmidt, T.; Chassé, T. Island Shapes and Aggregation Steered by the Geometry of the Substrate Lattice. *Chem. Commun. (Cambridge, U. K.)* **2012**, *48*, 6957−6959.
(32) Savu, S. A.; Biddau, G.; Pardini, L.; Bula, R.; Bettinger, H. F.; Draxl, C.; Chasse, T.; Casu, M. B. Fingerprint of the Metal-to-Molecule Fractional Charge Transfer at the Metal/Organic Interface. *J. Phys. Chem. C* **2015**, *119*, 12538−12544.
(33) Stöhr, J.; Outka, D. A. Determination of Molecular Orientations on Surfaces from the Angular Dependence of near-Edge X-Ray-Absorption Fine-Structure Spectra. *Phys. Rev. B: Condens. Matter Mater. Phys.* **1987**, *36*, 7891−7905.
(34) Mattheus, C. C.; de Wijs, G. A.; de Groot, R. A.; Palstra, T. T. M. Modeling the Polymorphism of Pentacene. *J. Am. Chem. Soc.* **2003**, *125*, 6323−6330.
(35) Clancy, P. Application of Molecular Simulation Techniques to the Study of Factors Affecting the Thin-Film Morphology of Small-Molecule Organic Semiconductors. *Chem. Mater.* **2011**, *23*, 522−543.
(36) Anthony, J. E. Functionalized Acenes and Heteroacenes for Organic Electronics. *Chem. Rev.* **2006**, *106*, 5028−5048.
(37) Duhm, S.; Heimel, G.; Salzmann, I.; Glowatzki, H.; Johnson, R. L.; Vollmer, A.; Rabe, J. P.; Koch, N. Orientation-Dependent Ionization Energies and Interface Dipoles in Ordered Molecular Assemblies. *Nat. Mater.* **2008**, *7*, 326−332.
(38) Koch, N. Electronic Structure of Interfaces with Conjugated Organic Materials. *Phys. Status Solidi RRL* **2012**, *6*, 277−293.
(39) Krause, S.; Schöll, A.; Umbach, E. Interplay of Geometric and Electronic Structure in Thin Films of Diindenoperylene on Ag(111). *Org. Electron.* **2013**, *14*, 584−590.
(40) Kolata, K.; Breuer, T.; Witte, G.; Chatterjee, S. Molecular Packing Determines Singlet Exciton Fission in Organic Semiconductors. *ACS Nano* **2014**, *8*, 7377−7383.
(41) Mas-Torrent, M.; Rovira, C. Role of Molecular Order and Solid-State Structure in Organic Field-Effect Transistors. *Chem. Rev.* **2011**, *111*, 4833−4856.
(42) Casu, M. B.; Chassé, T. Photoelectron Spectroscopy Applications to Materials Science. In *Handbook of Spectroscopy*, 2nd ed.; Gaglitz, G., Moore, D. S.Wiley-VCH: Weinheim, Germany, 2014; DOI: 10.1002/9783527654703.ch45.
(43) Freund, H.-J.; Bigelow, R. W.; Börsch-Pulm, B.; Pulm, H. Configuration Interaction Study of Shake-up Structure Accompanying Core-Ionization of Substituted Aromatic Molecules in the Vapor and Condensed Phases: Nitrosobenzene, Diazobenzene Dioxide and the NO Dimer. *Chem. Phys.* **1985**, *94*, 215−233.
(44) Freund, H.-J.; Bigelow, R. W. Dynamic Effects in VUV- and XUV-Spectroscopy of Organic Molecular Solids. *Phys. Scr.* **1987**, *1987*, 50.
(45) Kakavandi, R.; Savu, S.-A.; Sorace, L.; Rovai, D.; Mannini, M.; Casu, M. B. Core-Hole Screening, Electronic Structure, and Paramagnetic Character in Thin Films of Organic Radicals Deposited on $SiO_2/Si(111)$. *J. Phys. Chem. C* **2014**, *118*, 8044−8049.
(46) Koch, N.; Vollmer, A.; Duhm, S.; Sakamoto, Y.; Suzuki, T. The Effect of Fluorination on Pentacene/Gold Interface Energetics and Charge Reorganization Energy. *Adv. Mater.* **2007**, *19*, 112−116.
(47) Wong, S. L.; Huang, H.; Huang, Y. L.; Wang, Y. Z.; Gao, X. Y.; Suzuki, T.; Chen, W.; Wee, A. T. S. Effect of Fluorination on the Molecular Packing of Perfluoropentacene and Pentacene Ultrathin Films on Ag (111). *J. Phys. Chem. C* **2010**, *114*, 9356−9361.
(48) Duhm, S.; Hosoumi, S.; Salzmann, I.; Gerlach, A.; Oehzelt, M.; Wedl, B.; Lee, T.-L.; Schreiber, F.; Koch, N.; Ueno, N.; Kera, S. Influence of Intramolecular Polar Bonds on Interface Energetics in Perfluoro-Pentacene on Ag(111). *Phys. Rev. B: Condens. Matter Mater. Phys.* **2010**, *81*, 045418.
(49) Sakamoto, Y.; Suzuki, T.; Kobayashi, M.; Gao, Y.; Fukai, Y.; Inoue, Y.; Sato, F.; Tokito, S. Perfluoropentacene: High-Performance

DOI: 10.1021/acsami.5b05622
ACS Appl. Mater. Interfaces 2015, 7, 19774−19780

p−n Junctions and Complementary Circuits with Pentacene. *J. Am. Chem. Soc.* **2004**, *126*, 8138−8140.
(50) Meyer zu Heringdorf, F.-J.; Reuter, M. C.; Tromp, R. M. Growth Dynamics of Pentacene Thin Films. *Nature* **2001**, *412*, 517−520.
(51) Götzen, J.; Käfer, D.; Wöll, C.; Witte, G. Growth and Structure of Pentacene Films on Graphite: Weak Adhesion as a Key for Epitaxial Film Growth. *Phys. Rev. B: Condens. Matter Mater. Phys.* **2010**, *81*, 085440.
(52) Breuer, T.; Witte, G. Epitaxial Growth of Perfluoropentacene Films with Predefined Molecular Orientation: A Route for Single-Crystal Optical Studies. *Phys. Rev. B: Condens. Matter Mater. Phys.* **2011**, *83*, 155428.
(53) Kowarik, S.; Gerlach, A.; Hinderhofer, A.; Milita, S.; Borgatti, F.; Zontone, F.; Suzuki, T.; Biscarini, F.; Schreiber, F. Structure, Morphology, and Growth Dynamics of Perfluoro-Pentacene Thin Films. *Phys. Status Solidi RRL* **2008**, *2*, 120−122.
(54) Goose, J. E.; First, E. L.; Clancy, P. Nature of Step-Edge Barriers for Small Organic Molecules. *Phys. Rev. B: Condens. Matter Mater. Phys.* **2010**, *81*, 205310.
(55) de Oteyza, D. G.; Barrena, E.; Ossó, J. O.; Sellner, S.; Dosch, H. Thickness-Dependent Structural Transitions in Fluorinated Copper-Phthalocyanine (F_{16}CuPc) Films. *J. Am. Chem. Soc.* **2006**, *128*, 15052−15053.
(56) Schuster, B.-E.; Basova, T. V.; Plyashkevich, V. A.; Peisert, H.; Chassé, T. Effects of Temperature on Structural and Morphological Features of CoPc and CoPcF16 Thin Films. *Thin Solid Films* **2010**, *518*, 7161−7166. Yang, J.; Yan, D. Weak Epitaxy Growth of Organic Semiconductor Thin Films. *Chem. Soc. Rev.* **2009**, *38*, 2634−2645.
(57) Marchetto, H.; Groh, U.; Schmidt, T.; Fink, R.; Freund, H. J.; Umbach, E. Influence of Substrate Morphology on Organic Layer Growth: PTCDA on Ag(111). *Chem. Phys.* **2006**, *325*, 178−184.
(58) Ikonomov, J.; Bauer, O.; Sokolowski, M. Highly Ordered Thin Films of Perylene-3,4,9,10-Tetracarboxylic Acid Dianhydride (PTCDA) on Ag(100). *Surf. Sci.* **2008**, *602*, 2061−2068.
(59) Ikonomov, J.; Schmitz, C. H.; Sokolowski, M. Diffusion-Limited Island Decay of PTCDA on Ag(100): Determination of the Intermolecular Interaction. *Phys. Rev. B: Condens. Matter Mater. Phys.* **2010**, *81*, 195428.
(60) Dürr, A.; Koch, N.; Kelsch, M.; Rühm, A.; Ghijsen, J.; Johnson, R.; Pireaux, J. J.; Schwartz, J.; Schreiber, F.; Dosch, H.; Kahn, A. Interplay between Morphology, Structure, and Electronic Properties at Diindenoperylene-Gold Interfaces. *Phys. Rev. B: Condens. Matter Mater. Phys.* **2003**, *68*, 115428.
(61) Kowarik, S.; Gerlach, A.; Sellner, S.; Schreiber, F.; Cavalcanti, L.; Konovalov, O. Real-Time Observation of Structural and Orientational Transitions during Growth of Organic Thin Films. *Phys. Rev. Lett.* **2006**, *96*, 125504.
(62) Chkoda, L.; Schneider, M.; Shklover, V.; Kilian, L.; Sokolowski, M.; Heske, C.; Umbach, E. Temperature-Dependent Morphology and Structure of Ordered 3,4,9,10-Perylene-Tetracarboxylicacid-Dianhydride (Ptcda) Thin Films on Ag(1 1 1). *Chem. Phys. Lett.* **2003**, *371*, 548−552.
(63) Karl, N. Charge Carrier Transport in Organic Semiconductors. *Synth. Met.* **2003**, *133−134*, 649−657.
(64) Umbach, E.; Glöckler, K.; Sokolowski, M. Surface "Architecture" with Large Organic Molecules: Interface Order and Epitaxy. *Surf. Sci.* **1998**, *402−404*, 20−31.
(65) Ikonomov, J.; Bauer, O.; Sokolowski, M. Highly Ordered Thin Films of Perylene-3,4,9,10-Tetracarboxylic Acid Dianhydride (PTCDA) on Ag(100). *Surf. Sci.* **2008**, *602*, 2061−2068.
(66) Kilian, L.; Hauschild, A.; Temirov, R.; Soubatch, S.; Scholl, A.; Bendounan, A.; Reinert, F.; Lee, T. L.; Tautz, F. S.; Sokolowski, M.; Umbach, E. Role of Intermolecular Interactions on the Electronic and Geometric Structure of a Large π-Conjugated Molecule Adsorbed on a Metal Surface. *Phys. Rev. Lett.* **2008**, *100*, 136103.
(67) Huang, H.; Sun, J.-T.; Feng, Y. P.; Chen, W.; Wee, A. T. S. Epitaxial Growth of Diindenoperylene Ultrathin Films on Ag(111) Investigated by LT-STM and LEED. *Phys. Chem. Chem. Phys.* **2011**, *13*, 20933−20938.
(68) Jones, B. A.; Ahrens, M. J.; Yoon, M.-H.; Facchetti, A.; Marks, T. J.; Wasielewski, M. R. High-Mobility Air-Stable n-Type Semiconductors with Processing Versatility: Dicyanoperylene-3,4:9,10-Bis(Dicarboximides). *Angew. Chem., Int. Ed.* **2004**, *43*, 6363−6366.
(69) Weitz, R. T.; Amsharov, K.; Zschieschang, U.; Villas, E. B.; Goswami, D. K.; Burghard, M.; Dosch, H.; Jansen, M.; Kern, K.; Klauk, H. Organic n-Channel Transistors Based on Core-Cyanated Perylene Carboxylic Diimide Derivatives. *J. Am. Chem. Soc.* **2008**, *130*, 4637−4645.
(70) Lin, Y.; Zhan, X. Non-Fullerene Acceptors for Organic Photovoltaics: An Emerging Horizon. *Mater. Horiz.* **2014**, *1*, 470−488.
(71) Musumeci, C.; Salzmann, I.; Bonacchi, S.; Röthel, C.; Duhm, S.; Koch, N.; Samorì, P. The Relationship between Structural and Electrical Characteristics in Perylenecarboxydiimide-Based Nanoarchitectures. *Adv. Funct. Mater.* **2015**, *25*, 2501−2510.
(72) Ciccullo, F.; Savu, S. A.; Gerbi, A.; Bauer, M.; Ovsyannikov, R.; Cassinese, A.; Chasse, T.; Casu, M. B. Chemisorption, Morphology, and Structure of a n-Type Perylene Diimide Derivative at the Interface with Gold: Influence on Devices from Thin Films to Single Molecules. *Chem.−Eur. J.* **2015**, *21*, 3766−3771.
(73) Rivnay, J.; Jimison, L. H.; Northrup, J. E.; Toney, M. F.; Noriega, R.; Lu, S.; Marks, T. J.; Facchetti, A.; Salleo, A. Large Modulation of Carrier Transport by Grain-Boundary Molecular Packing and Microstructure in Organic Thin Films. *Nat. Mater.* **2009**, *8*, 952−958.
(74) Yoo, B.; Jung, T.; Basu, D.; Dodabalapur, A.; Jones, B. A.; Facchetti, A.; Wasielewski, M. R.; Marks, T. J. High-Mobility Bottom-Contact n-Channel Organic Transistors and Their Use in Complementary Ring Oscillators. *Appl. Phys. Lett.* **2006**, *88*, 082104.
(75) Jones, B. A.; Facchetti, A.; Wasielewski, M. R.; Marks, T. J. Effects of Arylene Diimide Thin Film Growth Conditions on n-Channel OFET Performance. *Adv. Funct. Mater.* **2008**, *18*, 1329−1339.
(76) Liscio, F.; Milita, S.; Albonetti, C.; D'Angelo, P.; Guagliardi, A.; Masciocchi, N.; Della Valle, R. G.; Venuti, E.; Brillante, A.; Biscarini, F. Structure and Morphology of PDI8-CN2 for n-Type Thin-Film Transistors. *Adv. Funct. Mater.* **2012**, *22*, 943−953.
(77) Youn, J.; Dholakia, G. R.; Huang, H.; Hennek, J. W.; Facchetti, A.; Marks, T. J. Influence of Thiol Self-Assembled Monolayer Processing on Bottom-Contact Thin-Film Transistors Based on n-Type Organic Semiconductors. *Adv. Funct. Mater.* **2012**, *22*, 1856−1869.
(78) Barra, M.; Girolamo, F. V. D.; Chiarella, F.; Salluzzo, M.; Chen, Z.; Facchetti, A.; Anderson, L.; Cassinese, A. Transport Property and Charge Trap Comparison for n-Channel Perylene Diimide Transistors with Different Air-Stability. *J. Phys. Chem. C* **2010**, *114*, 20387−20393.
(79) Liscio, F.; Albonetti, C.; Broch, K.; Shehu, A.; Quiroga, S. D.; Ferlauto, L.; Frank, C.; Kowarik, S.; Nervo, R.; Gerlach, A.; Milita, S.; Schreiber, F.; Biscarini, F. Molecular Reorganization in Organic Field-Effect Transistors and Its Effect on Two-Dimensional Charge Transport Pathways. *ACS Nano* **2013**, *7*, 1257−1264.

DOI: 10.1021/acsami.5b05622
ACS Appl. Mater. Interfaces 2015, 7, 19774−19780